Journal of Molecular Structure 1200 (2020) 127107

Contents lists available at ScienceDirect

Journal of Molecular Structure

journal homepage: http://www.elsevier.com/locate/molstruc

Optical, electrochemical, thermal, biological and theoretical studies of some chloro and bromo based metal-salophen complexes

Zohreh Shaghaghi [a, *], Nafis Kalantari [a], Mina Kheyrollahpoor [a], Mehri Haeili [b]

[a] Coordination Chemistry Research Laboratory, Department of Chemistry, Faculty of Science, Azarbaijan Shahid Madani University, P.O. box 83714-161, Tabriz, Iran
[b] Department of Biology, Faculty of Natural Science, University of Tabriz, P. O. box 5166616471, Tabriz, Iran

ARTICLE INFO

Article history:
Received 30 September 2018
Received in revised form
7 September 2019
Accepted 20 September 2019
Available online 21 September 2019

Keywords:
Metal-salophen complexes
DFT calculations
Antibacterial activity
Fluorescence spectroscopy
Cyclic voltammetry

ABSTRACT

Copper, cobalt and zinc-salophen complexes **3**–**8** were prepared from the reaction of N,N-bis(salicylidene)4-chloro-1,2-phenylendiamine (**1**) or N,N-bis(salicylidene)4-bromo-1,2-phenylendiamine (**2**) with their respective acetate salts. All compounds were characterized with common techniques. In additional, optical, electrochemical, thermal and antibacterial properties of ligands and their complexes were studied. Schiff base ligands **1** and **2** showed the intense emission band at 476 nm in the fluorescence spectra. The emission process of these ligands is related to the excited state intramolecular proton transfer phenomenon (and also $\pi\rightarrow\pi^*$ transitions). In general, after the incorporation of copper, cobalt and zinc metal ions into the structure of ligands **1** and **2**, the emission intensity of the ligands totally quenched. It can be attributed to the changes in the conformational rigidity of the structure of ligands upon complexation. Thermal stability of complexes was proved by TGA analysis. The cyclic voltammogrames of Cu (II) complexes displayed quasi-reversible one electron Cu(II)/Cu(I) redox process, while those of their cobalt counterparts exhibited two reversible redox couples of Co(II)/Co(I) and Co(III)/Co(II). The investigation of antibacterial activity against Staphylococcus *aureus*, *Escherichia coli*, *Pseudomonas aeruginosa* and carbapenem &colistin resistant *Klebsiella pneumoniae* showed both Co(II) complexes **4** and **7** have remarkable antibacterial activity. The antibacterial effect of cobalt complexes against *K. pneumoniae* is of high interest as the bacterium, is resistant to two most important therapeutic options for treatment of multi-drug resistant Gram-negative bacteria, including polymyxins and carbapenems. Moreover, DFT investigations were performed to obtain a better understanding of structure of compounds **1**–**8**. The values of band gap energies revealed ability of all compounds for using in optical devices. Finally, the electronic spectra of compounds are analyzed by TD-DFT calculations at the B3LYP/6-311G level for Schiff base ligands and the B3LYP/LANL2DZ level for complexes.

1. Introduction

Salenes and salophens are one old and common class of diimine tetradendate ligands in coordination chemistry [1,2]. These ligands are easily prepared from condensation reaction of ethylenediamine and 1,2-phenylenediamine or their derivatives with salicylaldehyde. Salophen metal complexes are formed by the reaction of both main and transition metal ions. The preparation method of theses complexes is easy and simple. In general, the ligand with one N_2O_2 core coordinates to a metal ion in a deprotonated form. Therefore, these type ligands produce neutral metal complexes when coordinate with divalent transition metal ions [3]. These complexes show extensive applications in several fields. Some of these complexes show substantial catalytic activity in a variety of reactions such as oxidation, epoxidation, hydrogenation, hydroxylation and cycloaddition reaction of CO_2 to propylene oxide [4–11]. A variety of them exhibit special optical properties [12]. They also found applications as electroluminescent materials [13,14] and biological activities such as antifungal, antibacterial, antimicrobial and interaction with DNA and RNA [15–20]. Metal salophen complexes show a tendency for square-planer geometry. They act as the bridge between the two imine groups. Therefore, two axial positions are available for coordinating solvent molecules or other donating groups. This makes them suitable for interaction with anions.

---

[*] Corresponding author.
E-mail address: shaghaghi@azaruniv.ac.ir (Z. Shaghaghi).

https://doi.org/10.1016/j.molstruc.2019.127107
0022-2860/

Anions as Lewis acid can donate one lone pair electron to the metal center. So, these compounds can be used as anion receptors [21–23].

Salen and salophen complexes with non-redox active zinc(II) metal ion can behave as interesting binders towards DNA structures [24,25]. In some cases, the metal center displays five coordinate square-pyramidal geometry. Salophens occupy the basal plane while a solvent molecule occupies the apical position. The zinc salophen complexes are known to be fluorescent and can be used as chemosensors for anions or selective receptors for other donating groups such as amines [26–29]. Also, the lack of redox activity of theses complexes produces species with low cytotoxicity. This makes suitable them for using as biological fluorescence probes [16].

Coordination cobalt complexes with salen or salophen type ligands have a low-spin configuration with a square planar donor atom symmetry. It has been proved that these complexes can act as catalysts for electroreduction of oxygen that is an important cathodic reaction in fuel cells and light-driven water oxidation [30,31]. Recently, the electrocatalytic activity of one bioinspired ionic liquid tagged Co-salophen metal complex has been demonstrated towards oxidation of glucose by Senthilkumar and coworkers [32]. Also, Khoshro et al. [33] have been investigated the electrochemical carboxylation of benzyl bromide by some cobalt (II) salophen type complexes. They found that the electrocatalytic reduction mechanism of benzyl bromide is depended on the electronic structure of the complexes.

Copper salophen complexes behaves as on-off light switch by multi-fold fluorescence enhancement or quenching upon saturation, are excellent DNA interacting system [34,35].

Density functional theory is a useful tool for studying the structural and electronical properties of metal complexes with organic ligands. The geometry optimization, electronic structures and theoretical assignments of the UV/Vis spectra of some salen and salophen complexes have been performed using DFT and TD-DFT methods in the literature. For example, Cisterna et al. [36] have been investigated electrochemical and theoretical properties of a series of neutral Ni(II) and copper(II) complexes with unsymmetrically-substituted N_2O_2-tetradentate Schiff-base ligands. They analyzed the electronic structures of the complexes using DFT and TD-DFT calculations. Consiglio and coworkers have been reported a computational study of the dimerization process of an amphiphilic Schiff-base bis (salicyladiminato)zinc(II) complex. They performed a comparative investigation between experimental and calculated ^{1}H NMR and UV–Vis spectra to evaluate the percentage contribute of each conformer [37]. Recently, the structure of a new mononuclear Co(II) salophen-type complex and optimizing of optimized of the molecular geometry in the ground state by DFT/(U)PBE0/Def2-TZVP level of theory have been reported by Zarei [38].

In view of the above mentioned factors, the purpose of the present work is to prepare and investigate some important structural properties of a series of salophen type complexes with different substitutions for their ability to be used in several fields such as precursors for preparation of metal oxide nanostructures, photovoltaic, electrocatalytic (water oxidation) and catalytic applications for future works. So, we report on synthesis and spectral characterization of two salophen-type ligands **1** and **2** resulting from condensation reaction of salicylaldehyde and 4-chloro-1,2-diaminobenzen or 4-bromo-1,2-diaminobenzen, respectively, and on Cu(II) complexes **3** [39] and **6**, Co(II) complexes **4** [39] and **7** and Zn(II) complexes **5** and **8** by treatment ligands **1** and **2** with copper, cobalt or zinc acetate salts, respectively. The optical, redox, thermal and antibacterial behavior of all ligands and complexes have been investigated. In additional, to investigate the potential use of complexes **3**–**8** in optical devices, the band gaps have been calculated at the DFT level, Finally, the obtained results are correlated with the experimental data.

2. Experimental

2.1. General procedures

All of solvents and materials were used without further purifications. NMR spectra were recorded on a Bruker Avance DPX-400 MHz spectrometer. FT-IR spectra were prepared with a FT-IR Spectrometer Bruker Tensor 27 after mixing the samples with KBr. Electronic absorption spectra were obtained with T 60 UV/vis Spectrometer PG Instruments Ltd. Fluorescence spectra were carried out using a FP-6200 spectrofluorometer (JASCO Corporation, Tokyo, Japan, http://www.jasco.co.jp). Cyclic valtammograms were recorded using an AUTOLAB PGSTAT-100 (potentiostat/galvanostat). Thermogravimetric analysis (TGA) were done by a Perkinelemersta 6000. Finally, C.H.N analyses were performed on ElementarVario ELIII.

2.2. General method for the preparation of salophen ligands

4-chloro-1,2-diaminobenzene (1.00 g, 7.00 mmol) or 4-bromo-1,2-diaminobenzene (0.500 g, 3.00 mmol) in 30 ml ethanol was slowly added to one ethanol solution of salicylaldehyde (1.49 ml, 14.0 mmol for chloro substitution and 0.568 ml, 6.00 mmol for bromo substitution) under stirring in room temperature. The solution turned to orange-brown and precipitate was appeared. The reaction continued for 4 h at room temperature. The precipitate was filtered and washed with ethanol and recrystallized in ethanol and then dried [39,40].

2.2.1. Synthesis of N,N-bis(salicylidene)4-chloro-1,2-phenylendiamine **(1)**

^{1}H NMR (400 MHz, DMSO-d_6): δ 12.77 (s, 1H, –OH), 12.69 (s, 1H,-OH), 8.99 (s, 1H, –HC=N-), 8.95 (s, 1H, –HC=N-), 7.69 (t, 2H, $J = 5.6$ Hz, Ar–H), 7.63 (d, 1H, $J = 2$ HZ, Ar–H), 7.52 (d, 1H, $J = 8.8$ Hz, ArH), 7.47 (d, $J = 2.0$ Hz, 1H, ArH), 7.45–7.42 (m, 2H, ArH), 7.02–6.97 (m, 4H, ArH); FT-IR (KBr, cm^{-1}), 3447, 1614, 1578, 1478, 1276, 1224, 1190, 1151,1115, 1085, 920, 866, 81, 752, 697, 652, 591, 503, 437; elem. Anal.: calc. for $C_{20}H_{15}N_2O_2Cl.0.5C_2H_5OH$: C, 67.47; N, 7.50; H, 4.81; found: C, 67.50; N, 7.90; H, 4.65; m.p: 138-141 °C; Yield: 67.96%.

2.2.2. Synthesis of N,N-bis(salicylidene)4-bromo-1,2-phenylendiamine **(2)**

^{1}H NMR (400 MHz, DMSO-d_6): δ 12.77 (s, 1H, –OH), 12.73 (s, 1H,-OH), 8.99 (s, 1H, –HC=N-), 8.95 (s, 1H, –HC=N-), 7.74 (d, 1H, $J = 5.6$ Hz, Ar–H), 7.69 (t, 2H, $J = 6.0$ Hz, Ar–H), 7.59 (dd, 1H, $J = 1.6$ Hz, ArH), 7.46–7.42 (m, 3H, ArH), 7.01–6.97 (m, 4H, ArH); FT-IR (KBr, cm^{-1}), 3446, 1614, 1577, 1475, 1458, 1384, 1277, 1191, 1151,1114, 913, 886, 837, 760, 647, 503; elem. Anal.: calc. for $C_{20}H_{15}N_2O_2Br.0.25C_2H_5OH.0.5H_2O$: C, 59.20; N, 6.74; H, 4.21; found: C, 59.49; N, 7.13; H, 4.63; m.p: 158-162 °C; Yield: 63.52%.

2.3. General method for the preparation of complexes **3**–**8**

To a stirring dichloromethane solution of ligand **1** (0.710 mmol) in 15 ml or **2** (0.630 mmol) in 10 ml, one ethanol solution of $Cu(CH_3COO)_2.1H_2O$, $Co(CH3COO)_2.4H_2O$ or $Zn(CH_3COO)_2.2H_2O$ (0.710 or 0.630 mmol) in 15 ml was slowly added at room temperature, Immediately, the color of solution turned and precipitate appeared. The reaction continued at room temperature for 4 h and then the precipitate was filtered and washed with ethanol. The

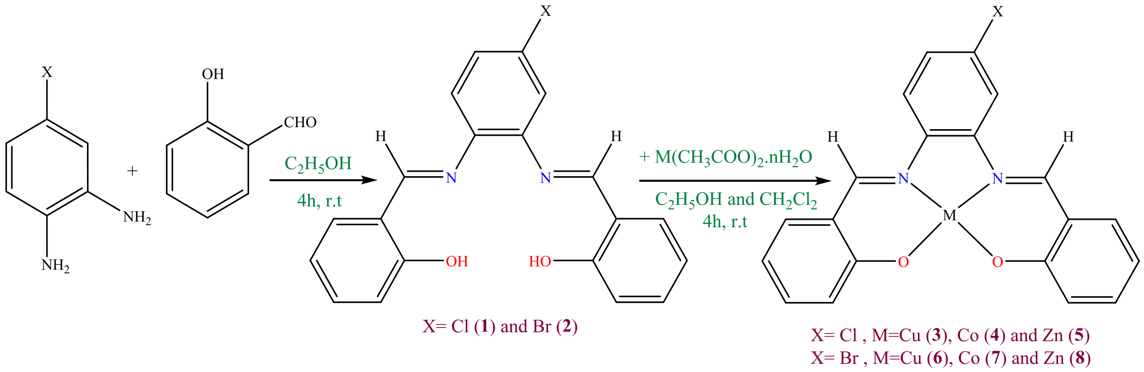

Scheme 1. The route of synthesis of salophen type ligands **1** and **2** and their Cu, Co and Zn complexes (**3**–**8**).

Table 1
Molar conductivity values for ligands and complexes (10^{-3} M in DMSO).

Compound	Molar conductivity ($Cm^2\ \Omega^{-1}mol^{-1}$)
DMSO	1.475
1	1.736
2	1.764
3	1.767
4	3.60
5	1.520
6	1.538
7	3.14
8	1.627

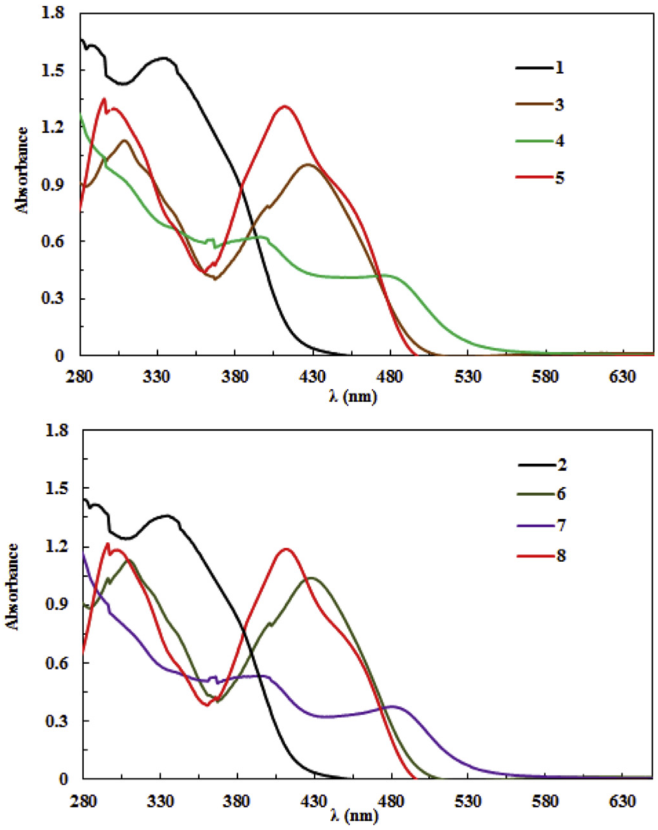

Fig. 1. UV–vis spectra of compounds **1**–**8**.

filtrated solid was recrystallized with ethanol-dichloromethane and dried under vacuum.

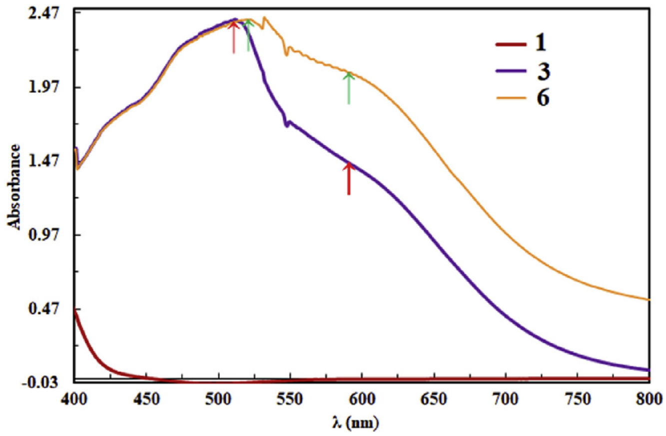

Fig. 2. d→d transitions of Cu complexes **3** and **6** (10^{-2} M in DMSO).

2.3.1. Cu(II) complex **3**

FT-IR (KBr, cm^{-1}), 3423, 1608, 1578, 1519, 1485, 1460, 1373, 1338, 1241, 1188, 1150, 1130, 1093, 938.901, 849, 803, 753, 548, 434; elem. Anal.: calc. for $CuC_{20}H_{13}N_2O_2Cl.0.25H_2O$: C, 57.62; N, 6.72; H, 3.24.; found: C, 57.47; N, 7.14; H, 3.65; Decomp: 300 °C; Yield: 64.10%.

2.3.2. Co(II) complex **4**

FT-IR (KBr, cm^{-1}), 3446, 1619, 1577, 1542, 1489, 1445, 1384, 1306, 1192, 1158, 1132, 1038, 948.901, 870, 814, 756, 696, 598, 567, 470; elem. Anal.: calc. for $CoC_{20}H_{13}N_2O_2Cl.2H_2O.1.5\ CH_2Cl_2$: C, 45.18; N, 4.90; H, 3.50.; found: C, 45.31; N, 4.61; H, 3.52; Decomp: 279 °C; Yield: 68.96%.

2.3.3. Zn(II) complex **5**

^{1}H NMR (400 MHz, DMSO-d_6): δ 9.07 (s, 1H, –HC=N-), 9.040 (s, 1H, –HC=N-), 8.064 (d, 1H, $J=2$ Hz, ArH), 7.95 (s, 1H, $J=9.2$ Hz, ArH), 7.46–7.42 (m, 3H, Ar–H), 7.30–7.26 (m, 2H, Ar–H), 6.72 (d, 2H, $J=8.4$ Hz, ArH), 6.54 (t, $J=8.0$ Hz, 2H, ArH); FT-IR (KBr, cm^{-1}), 3423, 1610, 1578, 1525, 1463, 1380, 1316, 1245, 1178, 1150, 1124, 1093, 1057, 930, 898, 852, 804, 751, 589, 540, 507, 424; elem. Anal.: calc. for $ZnC_{20}H_{13}N_2O_2Cl.2H_2O$: C, 53.35; N, 6.22; H, 3.77.; found: C, 53.55; N, 6.38; H, 3.21; Decomp: 330 °C; Yield: 65.00%.

2.3.4. Cu(II) complex **6**

FT-IR (KBr, cm^{-1}), 3423, 1607, 1571, 1521, 1458, 1372, 1328, 1249, 1187, 1149, 1128, 1080, 1050, 927, 888, 847, 801, 756, 682, 629, 573, 544, 500, 436; elem. Anal.: calc. for $CuC_{20}H_{13}N_2O_2Br.0.5H_2O.0.5CH_2Cl_2$: C, 48.42; N, 5.51; H, 2.95.; found: C, 48.09; N, 5.93; H, 3.01; m.p: 303–308 °C; Yield: 68.20%.

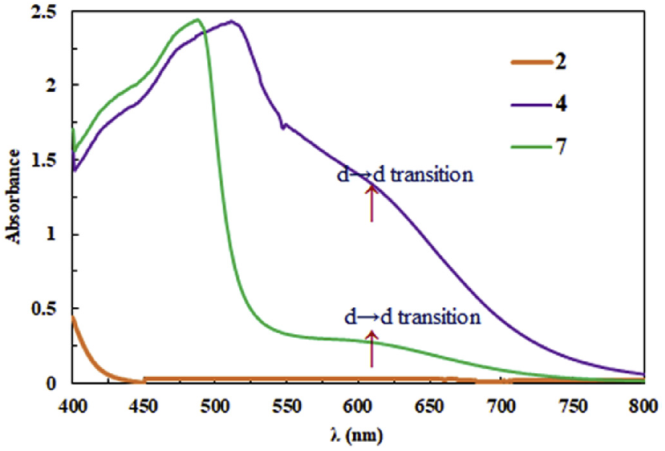

Fig. 3. d→d transitions of Co complexes **4** and **7**(10^{-2} M in DMSO).

2.3.5. *Co(II) complex **7***

FT-IR (KBr, cm^{-1}), 3446, 1610, 1578, 1525, 1463, 1380, 1316, 1245, 1178, 1150, 1124, 1093, 1057, 930, 898, 852, 804, 751, 589, 540, 507, 424; elem. Anal.: calc. for $CoC_{20}H_{13}N_2O_2Br.2H_2O. CH_2Cl_2$: C, 43.97; N, 4.89; H, 3.31.; found: C, 43.84; N, 4.53; H, 2.69; m.p: 289-293 °C; Yield: 65.20%.

2.3.6. *Zn(II) complex **8***

^{1}H NMR (400 MHz, DMSO-d_6): δ 9.08 (s, 1H, −HC═N-), 9.04 (s, 1H, −HC═N-), 8.17 (d, 1H, *J* = 1.2 Hz, ArH), 7.87 (d, 1H, *J* = 8.8 Hz, ArH), 7.54 (d, *J* = 8.7 Hz, 1H, Ar−H), 7.44 (dd, *J* = 7.2 Hz, 2H, Ar−H), 7.27 (t, 2H, *J* = 8.0 Hz, ArH), 6.7 (d, 2H, *J* = 8.8 Hz, ArH), 6.55−6.51 (m, 2H, ArH); FT-IR (KBr, cm^{-1}), 3422, 1610, 1573, 1529, 1460, 1444, 1381, 1321, 1243, 1178, 1151, 11126, 1030, 969, 923, 889, 852, 805, 752, 680, 621, 538, 490; elem. Anal.: calc. for $ZnC_{20}H_{13}N_2O_2Br.2.5H_2O.2C_2H_5OH.$: C, 48.37; N, 4.70; H, 5.03.; found: C, 48.59; N, 4.23; H, 5.43; Decomp: 338 °C; Yield: 69.50%.

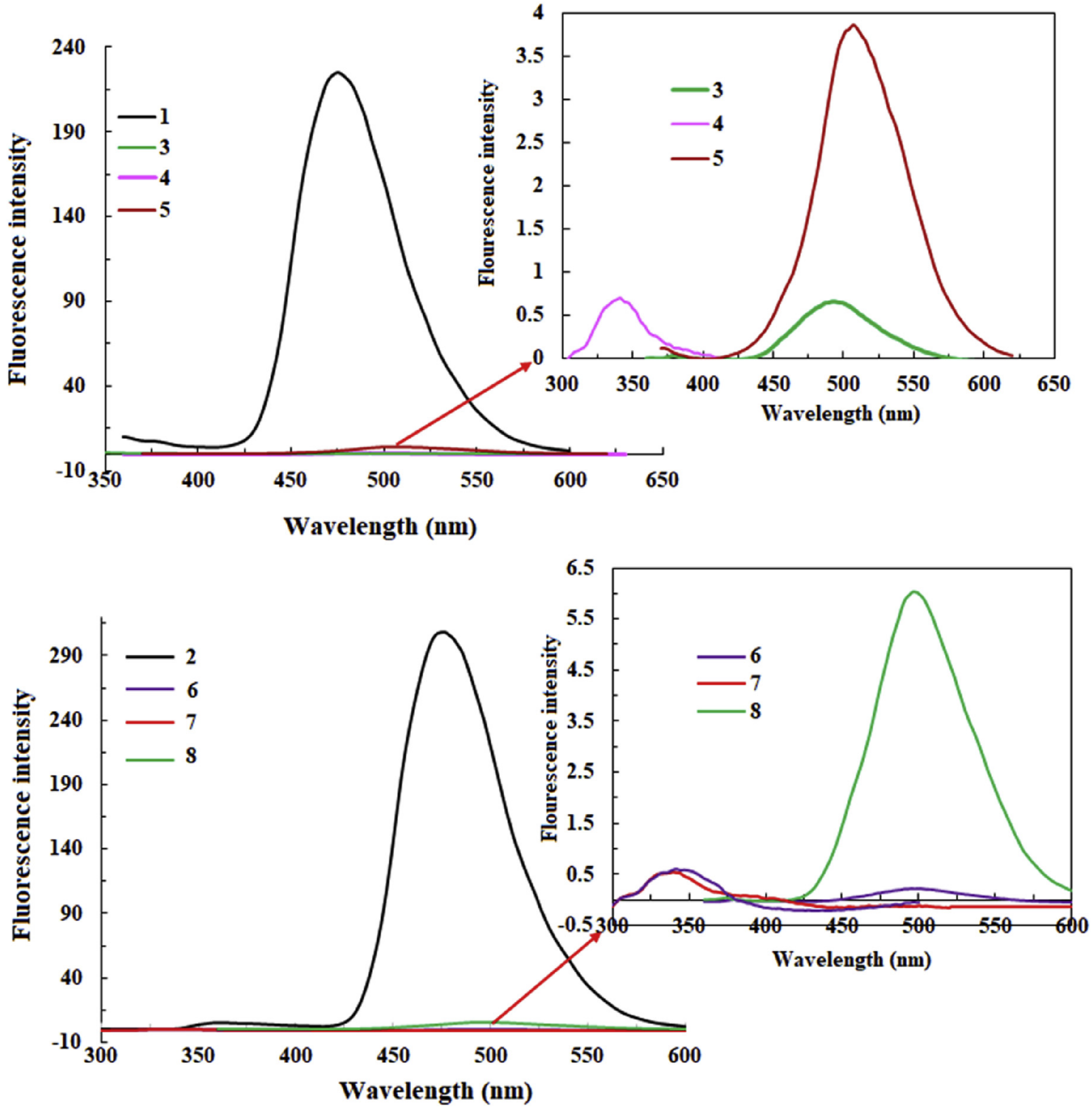

Fig. 4. Fluorescence spectra of compounds **1**–**8**.

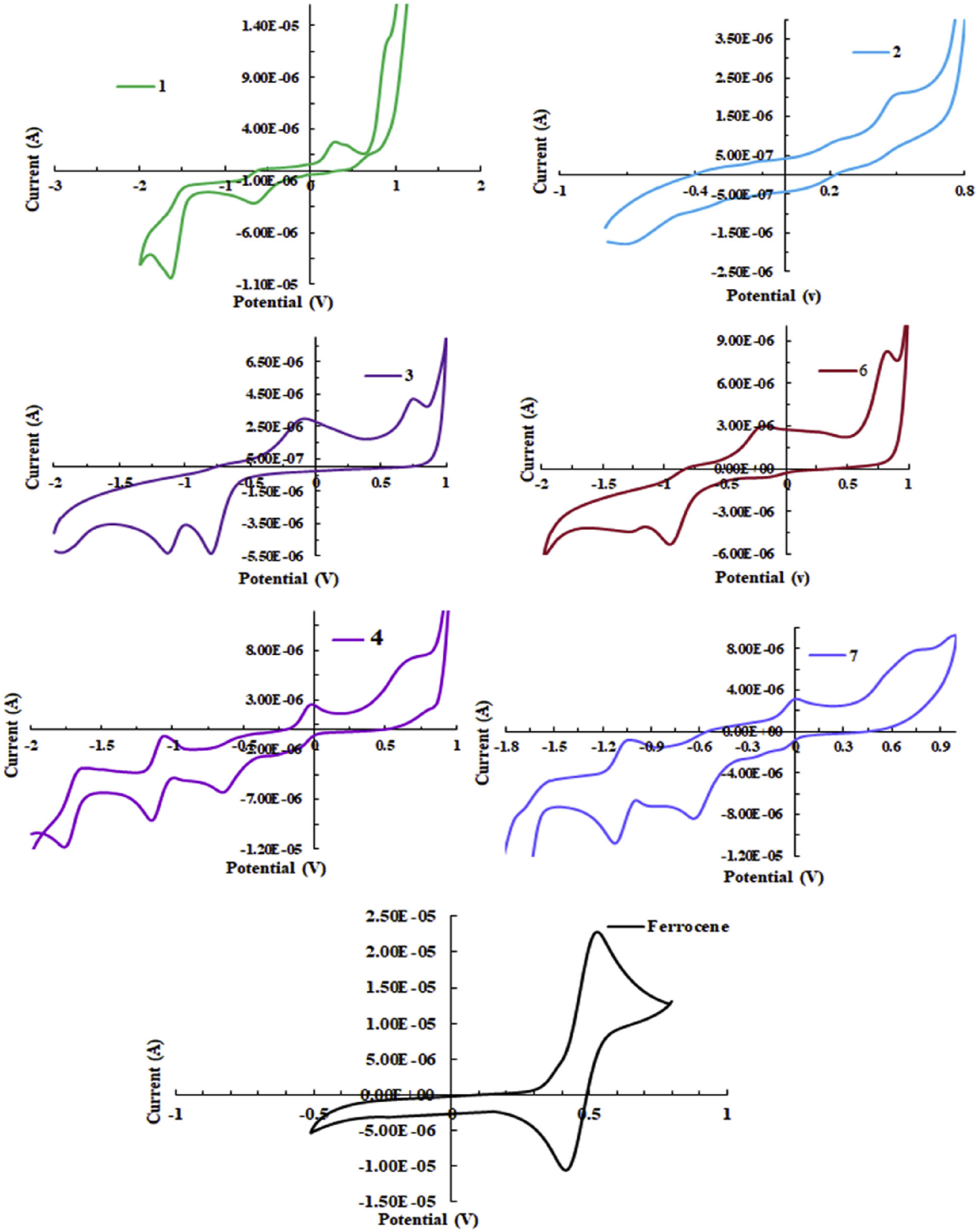

Fig. 5. Cyclic voltammograms of ligands **1** and **2** and their Cu and Co complexes recorded in DMSO, internal reference: $Cp_2Fe^{0/+}$.

2.4. *Evaluation of antibacterial activity*

The test microorganisms; *Staphylococcus aureus*, *Escherichia coli*, *Pseudomonas aeruginosa* and carbapenem & colistin resistant *Klebsiella pneumoniae* were maintained on Nutrient agar slants agar slop at 4 °C and sub-cultured for 24 h before use. The antibacterial activity of ligands and their complexes in DMSO was evaluated in vitro by agar well diffusion method. Ceftriaxone and DMSO were

Table 2
Electrochemical data for ligands **1** and **2** and their complexes with Cu (**3** and **6**) and Co (**4** and **7**).

Compound	E_{pa}(V)	E_{pc}(V)	$E_{1/2}$/V (ΔEp (mV))
Ferrocene	0.528	0.417	0.472 (111)
1	0.306	−1.63	–
	−0.550	−0.630	0.590 (80.0)
2	0.489	−0.679	–
	0.237	0.116	0.176 (121)
3	−0.086	−0.790	−0.438 (704)
	0.769	−1.12	–
4	−1.08	−1.14	−1.11 (57.0)
	0.014	−0.066	−0.026 (80.5)
	0.668	−0.645	–
6	−0.230	−0.959	0.594 (729)
	0.764	–	–
7	−1.07	−1.12	−1.09 (53.0)
	0.007	−0.066	−0.029 (73.0)
	0.744	−0.628	–

used as positive and negative controls for the antibacterial susceptibility testing respectively. All compounds were dissolved in 300 μl DMSO, except for compound **3** which was dissolved in 500 μl. Then 60 μl of each reconstituted compound was transferred to each well measuring 5.5 mm in diameter.

2.5. Electrochemical experiments

The electrochemical properties of Schiff base ligands **1** and **2** and their complexes with copper and cobalt ions were investigated by cyclic voltammetry. Cyclic voltammetry (CV) was performed using the solutions of ligands and complexes (10 ml, 10^{-3} M) prepared in DMSO with 0.1 M $LiClO_4$ as a supporting electrolyte and using a glassy carbon working electrode, a Ag/AgCl reference electrode and a Pt wire counter electrode under N_2 atmosphere at room temperature. The potential was scanned in the range of +1.50 to −1.50 V at 50 mV/s potential scan rate.

2.6. Theoretical studies

DFT calculations were carried out using Gaussian 09 version D.01 program package [41]. Initial structures of all compounds were drawn in the Gaussian software. Molecular structures were optimized using the B3LYP (Becke's Three parameter Hybrid Functional Using the LYP Correlation Functional) approach in conjunction with the 6-311G basis set for Schiff base ligands and the LANL2DZ basis set for complexes [42]. No symmetry cbonstrains were applied during the geometry optimization. For calculating the excited state properties, time-dependent density functional theory (TDDFT) [43] was employed at the B3LYP/6-311G level for Schiff base ligands and the B3LYP/LANL2DZ level for complexes using dimethyl sulfoxide (DMSO) as solvent and the excitation energies, oscillator strengths and orbital contribution for the lowest 50 singlet-singlet transitions at the optimized geometry in the ground state were obtained.

3. Results and discussions

3.1. Synthesis and characterization

Ligands **1** and **2** were synthesized by condensation reaction of salicylaldehyde and 4-chloro-1,2-diaminobenzene or 4-bromo-1,2-diaminobenzene in ethanol at room temperature for 4 h. The complexes **3**–**8** were prepared by reacting ligands **1** and **2** in CH_2Cl_2 and 1 equiv. of Cu(II), Co(II) and Zn(II) acetate salts in ethanol (Scheme 1).

3.1.1. FT-TR spectra

In the IR spectra of the schiff-base ligands, a sharp and strong band is observed at 1614 cm^{-1}, which is assigned to the absorption of imine stretching vibration. Compounds **1** and **2** also display one strong and broad band at 3448 and 3450 cm^{-1} that can be related to the stertching vibrations of phenolic hydroxyl groups (and also water molecules). The ν(-C═C-) stretching vibrations of aromatic rings appear at the range of 1473–1578 cm^{-1}. Additionally the observed peaks between 752 and 822 cm^{-1} are assigned to the bromine and chlorine (Figs. S1 and S2) [44,45]. After complexation with copper, cobalt and zinc metal ions, the absorbance of imine

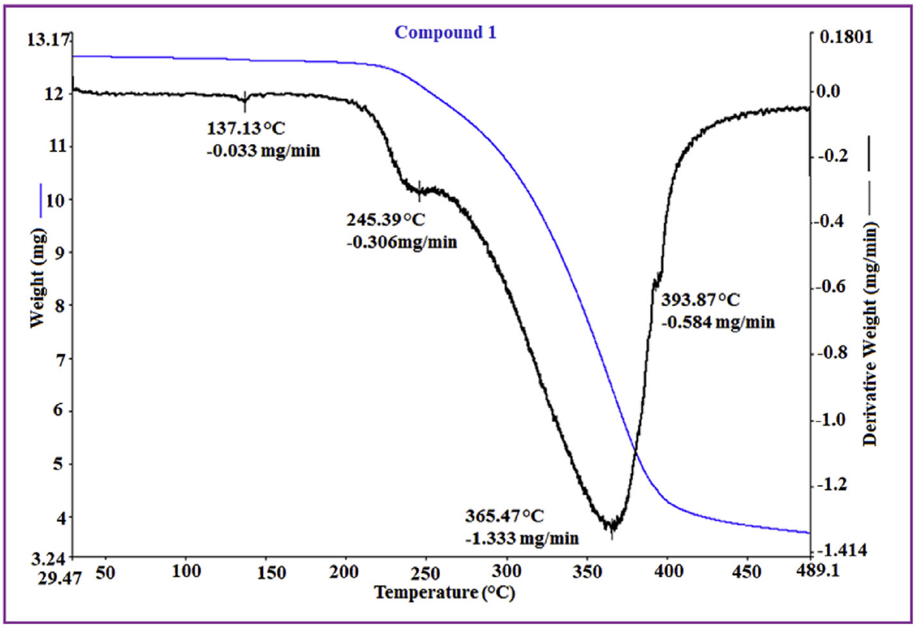

Fig. 6. The thermogravimetric plots of Schiff-base ligands **1** and **2** as weight loss versus temperature.

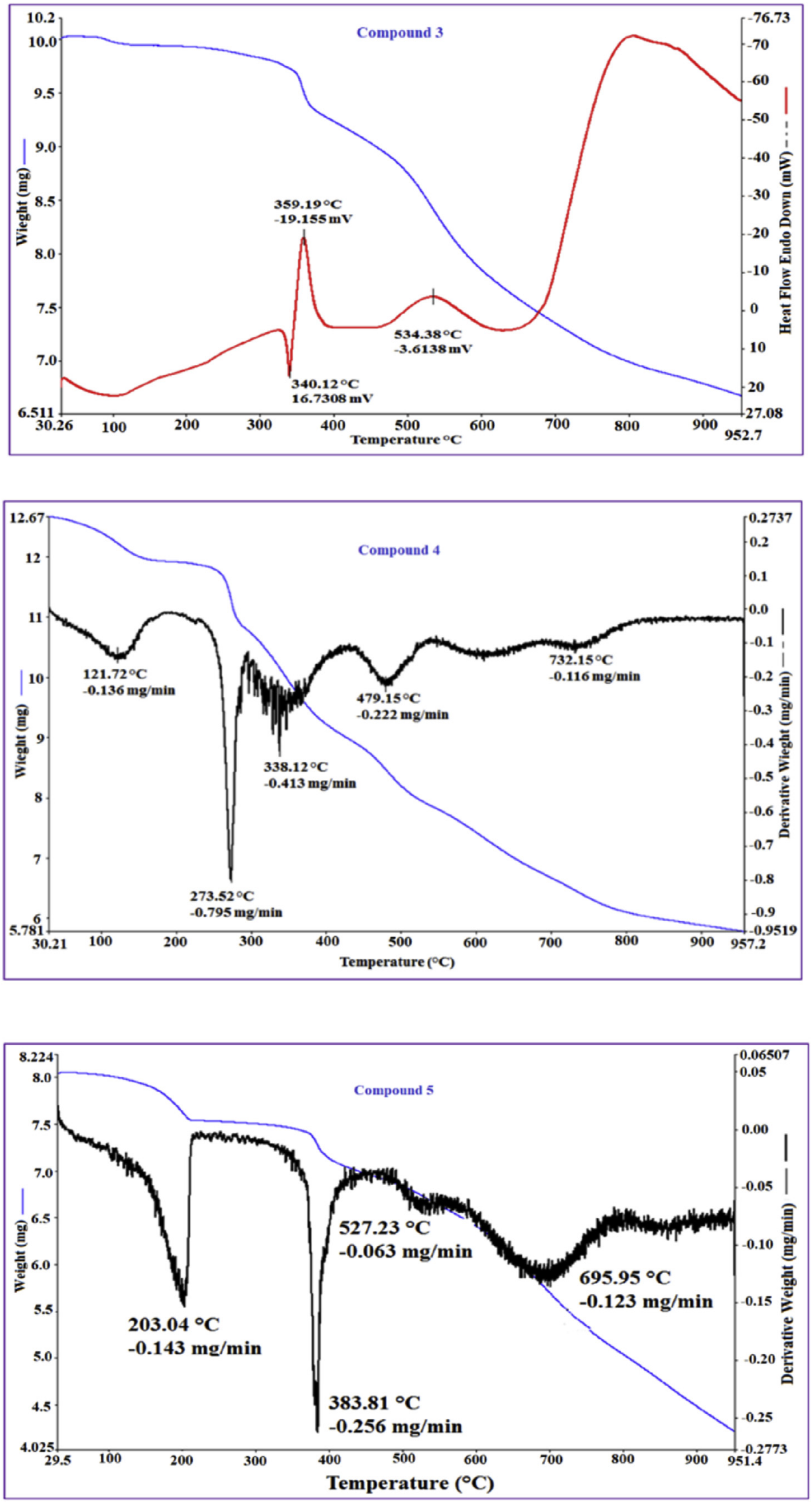

Fig. 7. The thermogravimetric plots of Cu(II), Co(II) and Zn(II) complexes of ligand **1** (**3**–**5**).

Table 3
The results of antibacterial activity of the tested compounds, presented as diameter of the zone of inhibition (mm).

Compound	*S. aureus*	*E. coli*	*P. aeruginosa*	carbapenem &colistin resistant *K. pneumoniae*
1	21	16	13	10
2	19	13	13	15
3	No halo	15	10	No halo
4	27	20	27	23
5	No halo	13	10	11
6	No halo	13	10	No halo
7	22	16	19	17
8	10	13	9.5	No halo

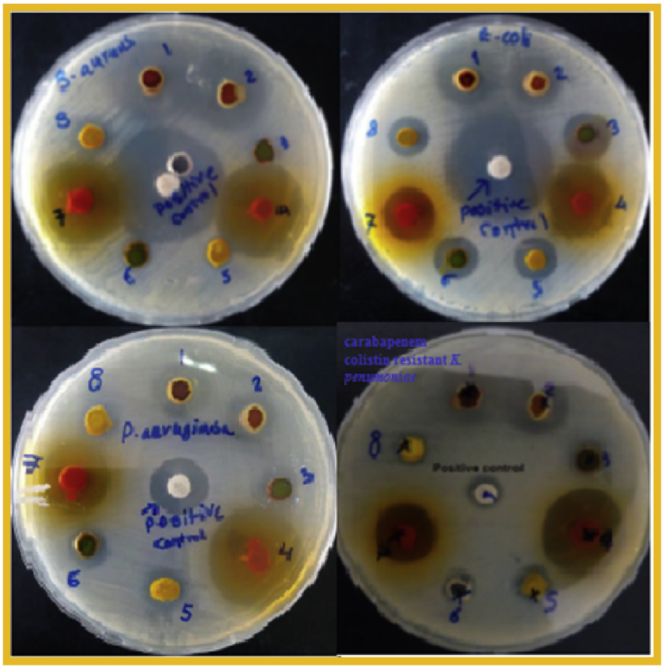

Fig. 8. Diameter of the zone of inhibition of compounds **1**–**8** against studied bacteria (*Staphylococcus aureus*, *Escherichia coli*, *Pseudomonas aeruginosa* and carbapenem &colistin resistant *Klebsiella pneumoniae*.

vibrations shifts to shorter or higher wavenumbers about 5–8 cm^{-1}. In some cases, these bands decrease in intensity after complexation. This suggests the coordination of electron pair of nitrogen atoms of imine groups to the metal ion center. The broad and strong bands around 3446 and 3422 cm^{-1} in the spectra of complexes probably corresponds to the H_2O stretching vibration. In additional, the ν (M-O) and ν (M-N) are identified in the range of 434–598 cm^{-1} [44,45]. Finally, the medium and weak peaks about 752–758 cm^{-1} and 803-850 cm^{-1} are related to the bromine and chlorine, respectively (Figs. S3–S8) [45].

3.1.2. ^{1}H NMR spectra

In the ^{1}H NMR spectra of ligands, two singlet resonances of two none-equivalent –OH protons appar at 12.70 ppm and 12.77 ppm in **1** and 12.74 ppm and 12.77 ppm in **2**, while two singlet resonances at approximately 8.95 ppm and 8.99 ppm are assigned to two non-eqivalent imine protons [46]. The aromatic protons of compounds **1** and **2** appear in the range of 6.97–7.74 ppm (Figs. S9 and S10).

As expected, the singlet resonances corresponding to the –OH groups are disappeared in the ^{1}H NMR spectra of Zn complexes **5** and **8**, This indicates the phenolic hydroxyl groups are deprotonated when bound to Zn(II) metal ion, Also, in the comparison with ligands, the imine proton resonances shift to downfield and appeared at approximately 9.04 ppm and 9.08 ppm which confirm the coordination of nitrogen atoms of imine groups to the Zn(II) metal ion center [44,47,48]. Moreover, the aromatic protons are observed at 6.51–8.18 ppm (Figs. S11 and S12).

3.2. Molar conductivity

The values of molar conductivity of all compounds are summerized in Table 1. The results show that all complexes are non-electrolyte. Therefore, ligand **1** and **2** act as one dianionic and tetradentate ligands with one N_2O_2 core when bound to the metal ion center (Scheme 1).

3.3. UV/vis spectroscopy

The UV/Vis spectra of all compounds are recorded in DMSO solution (10^{-4} M) and shown in Fig. 1. In general, the absorption spectra exhibit intense bands in the 264–338 nm region which can be related to the $\pi \rightarrow \pi^*$and $n \rightarrow \pi^*$ transitions of aromatic rings and azomethine bonds [44,45]. It should be noted that Schiff base ligands exhibit enolimine-ketoamine tautomers in solution [49]. There are several factors such as temperature, solvent, substitution and complexation that affect keto-enol equilibrium [50,51]. $\pi \rightarrow \pi^*$ transition of keto form is usually observed at wavelengths above 400 nm. Here, a low intensity broad shoulder which observed at around 400 nm, can be assigned to the ketoamine tautomer for ligands **1** and **2** [49,50]. As shown in Fig. 1, $n \rightarrow \pi^*$ transitions of imine groups decrease in intensity and shift to shorter wavelengths after complexation. Also, the absorption band of the enol forms of ligands disappear in the complexes. The phenolic hydroxyl groups are deprotonated when bound to the metal ion center. Therefore, there is no enolic proton in complexes. Consequently, the absorption bands which observed for copper complexes **3** and **6** at 427 nm, for cobalt complexes **4** and **7** at around 400 nm and 480 nm and for zinc complexes **5** and **8** at 412 nm and 450 nm can be assigned to the intra-ligand $\pi \rightarrow \pi^*$ transitions of keto tautomer of ligands [50]. On the other hand, MLCT or LMCT is a very common phenomenon in salophen type complexes that usually appears in the same region and cannot be ignored [3,44,45,52,53]. It is likely that charge transfer bands overlap with some of $d \rightarrow d$ bands or with the $\pi \rightarrow \pi^*$ transitions [54]. As we will discuss later, in the case of Cu(II) complexes and especially cobalt(II) complexes, TD-DFT calculations indicates that the absorption bands in the 400–500 nm region can also be related to the MLCT and LMCT, while theoretical data does not support it for Zn complexes. According to the literature, $d \rightarrow d$ transitions (lower energy bands) are observed in the range 540–650 nm for square-planner Cu(II) complexes [36,44]. The appearance of low intensity bands at 511 and 609 nm in **3** and 518 and 600 nm in **6** which related to the $d \rightarrow d$ transitions, may indicate square-planner structure for them. (Fig. 2). About Co(II) complexes **4** and **7**, the low intensity bands between 598 and 605 nm are

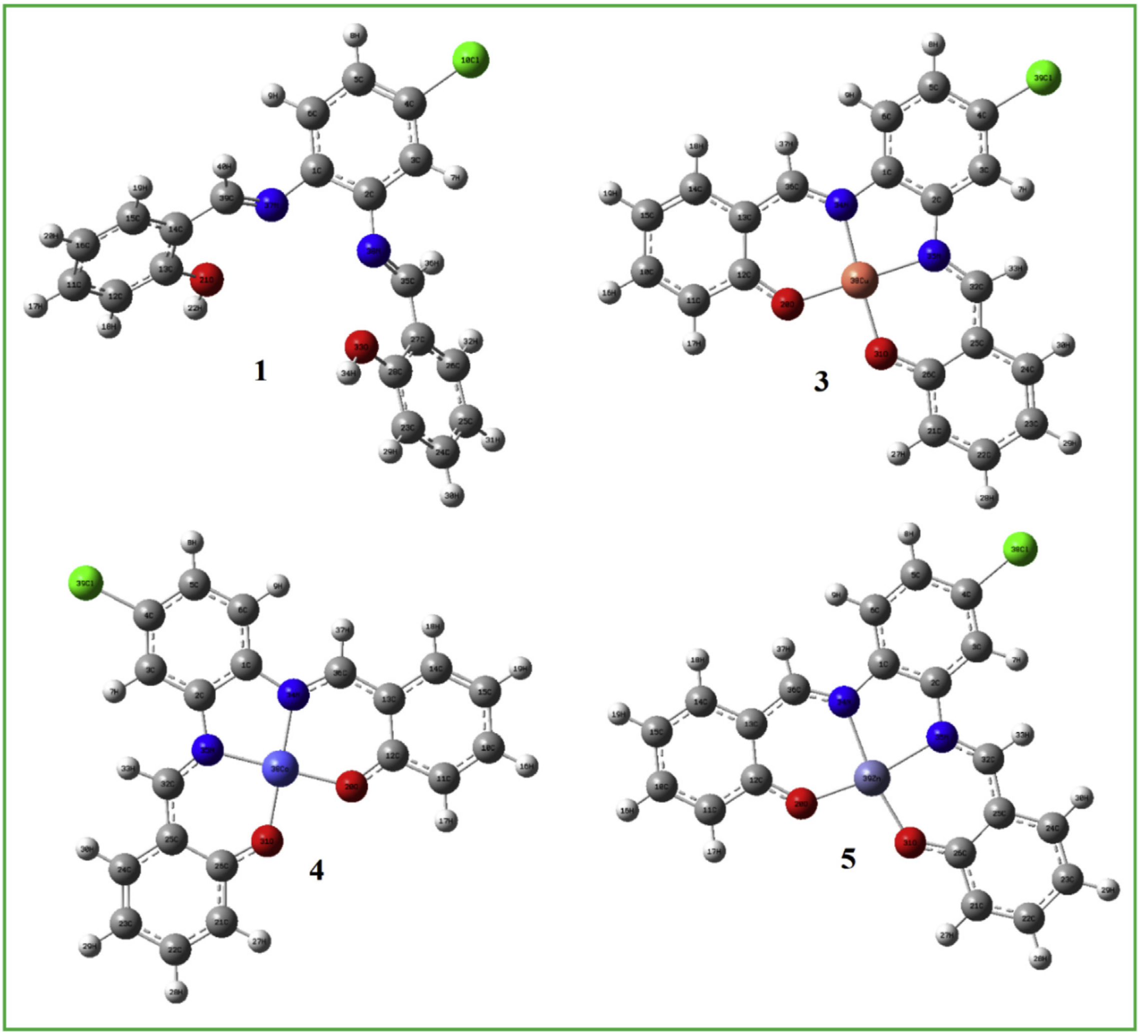

Fig. 9. Optimized geometries of Schiff-base ligand **1** and its complexes (**3**–**5**).

assigned to the d → d transitions (Fig. 3). Moreover, d → d transitions are not observed in the visible region for Zn(II) complexes **5** and **8** because of the d^{10} configuration of Zn(II) ion [55] (note that d → d transitions are forbidden and exhibit a small absorption coefficient and not seen in dilute solution of complexes (Fig. 1). Therefore, to observe these transitions, the stock solutions of complexes in DMSO were prepared).

3.4. Fluorescence study

The emission spectra of ligands and their complexes are given in Fig. 4. Ligands **1** and **2** exhibit a maximum emission peak at 476 nm upon excitation at 339 nm and 278 nm, respectively. According to the literature [49,50,56–58], the emission process of Schiff-base ligands is related to the $\pi \rightarrow \pi^*$ intra-ligand transitions which can be explained as follows: the excited state which formed by the $\pi \rightarrow \pi^*$ transition of enol form undergoes an ultrafast twist and proton transfer in the time of 100 fs. Then the twists enol for returns to ground state through a nonradiative manner. The formed *cis*-keto state, as a result of excited state proton transfer emit. The prominent bands in the fluorescence spectra of compounds **1** and **2** show Stokes shifts about 137 nm and 198 nm, respectively. In general, after the incorporation of copper, cobalt and zinc metal ions into the structure of both ligands, the emission intensity of ligands totally quenches. It should be noted that the absorption band of the enol form of ligands disappears in the complexes (Fig. 1) and there is no enolic proton. Consequently, the excited state intramolecular proton transfer (ESIPT) is not responsible for the emission intensity in contrast to the free ligands. According to the literature, it was expected that the absorption bands present in these complexes at 420–500 nm related to the intra-ligand $\pi \rightarrow \pi^*$ transitions of keto form of ligands and charge transfer transitions would be responsible for the emission in the complexes [50,59]. Surprisingly, we found that these complexes quench the fluorescence intensity of ligands, which means that none of the absorption peaks leads to a noticeable emission in the complexes compared to the free ligands. It seems that the incorporation of metal ions affects the conformational rigidity of the structure of ligands and almost quenches the fluorescence intensity [18]. Since, the complexes do not exhibit a significant emission, the expression of excitation and emission wavelengths is merely to compare the effect of different metal ions entering to the ligand structure. (For example, the typically excitation spectra for ligand **1** and complex **5** are given in Fig. S13).

3.5. Cyclic voltammetry

The electrochemical properties of Schiff-base ligands **1** and **2**

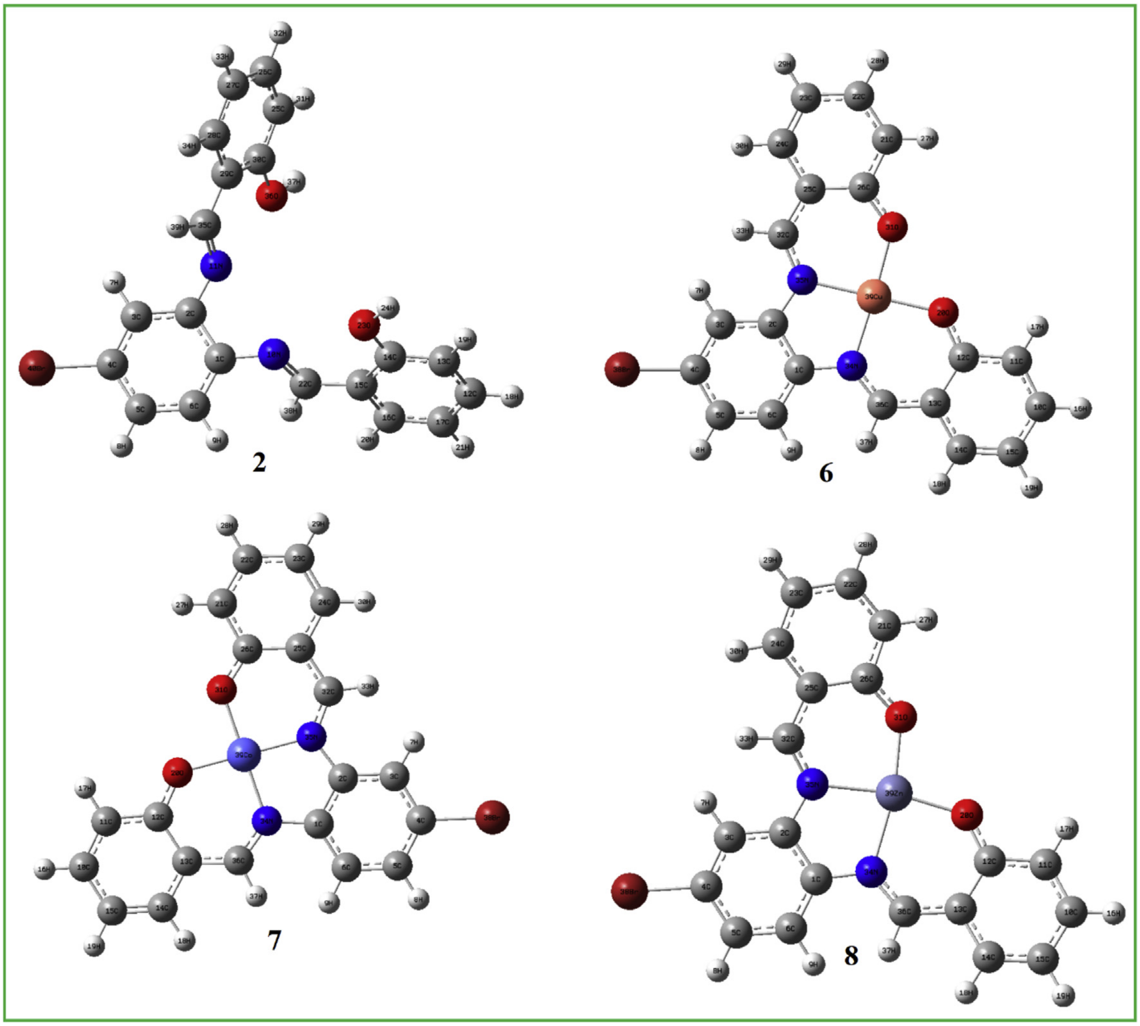

Fig. 10. Optimized geometries of Schiff-base ligand **2** and its complexes (**6**–**8**).

and their Cu(II) and Co(II) complexes are investigated using cyclic voltammetry in DMSO solutions containing 0.1 M $LiClO_4$ as a supporting electrode at room temperature in a potential range of +1.50 to −1.50 V at 50 mV/s potential scan rate. The cyclic voltammograms of ligands and complexes are shown in Fig. 5 and electrochemical data of all compounds summarized in Table 2. Cu(II) complexes **3** and **6** exhibit one electron quasi-reversible oxidation and reduction process [36,39]. The anodic wave which appeared in the range of −0.0860 to −0.230 V, assigned to the quasi-reversible electron oxidation of Cu(I) to Cu(II) while the chathodic wave in the range of −0.790 to −0.959 V is attributed to quasi-reversible electron reduction of Cu(II) to Cu (I). Moreover, the observed anodic wave at 0.769 V for **3** and 0.764 v for **6** corresponds to the oxidation of respective ligands. Finally, the observed cathodic wave at −1.12 V for **3** is assigned to the reduction of respective ligand. Both voltammograms of Co complexes **4** and **7** display two sets of redox peaks. The peaks at high negative potentials are assigned to Co(II)/Co(I) redox couple and the peaks at the less negative potentials are assigned to Co(II)/Co(III) redox couple [32,39,53,60]. For complex **4**, the anodic peak at −1.083 V and cathodic peak at −1.14 V are assigned to reversible redox couple Co(II)/Co(I) and oxidation wave at 0.014 V and reduction wave at −0.066 V are attributed to reversible redox couple Co(III)/Co(II). Additionally, the waves which observed at 0.668 V and −0.645 V in voltammogram of **4**, are assigned to the oxidation and reduction of respective ligand, respectively. About complex **7**, observed anodic and cathodic waves at −1.07 and −1.12 V are attributed to reversible redox couple Co(II)/Co(I) while observed anodic and cathodic waves at 0.007 and −0.066 V are related to reversible redox couple Co(III)/Co(II). Finally, the anodic and cathodic peaks at = 0.744 V and −0.628 V probably correspond to oxidation and reduction of respective ligand.

3.6. Thermogravimetric analysis

Thermogravimetric analysis (TGA) are used up to 900 °C at N_2 atmosphere to investigate the thermal stability of ligands **1** and **2** and Cu(II) (**3** and **6**), Co(II) (**4** and **7**) and Zn(II) (**5** and **8**) complexes. Ligands **1** and **2** are stable up to 200 °C with a DTGmax = 245 °C for **1** and 235 °C for **2**. The thermogravimetric plots of Schiff-base ligands **1** and **2** as weight loss versus temperature have been shown in Fig. 6 and Fig. S14. Thermal decomposition of ligands take places in two stages. The first stage is probably related to the omission of solvent molecule with a mass lose 6.49% (calc. 6.16%) for **1** and 3.15% (calc. 2.82%) for **2**. The second stage is related to vigorous decomposition of organic residues, with a mass loss of 64.30% (calc. 64.26%) for **1** and 61.33% (calc. 60.75%) for **2**.

The TGA plots of Cu(II) complexes **3** and **6** show both complexes

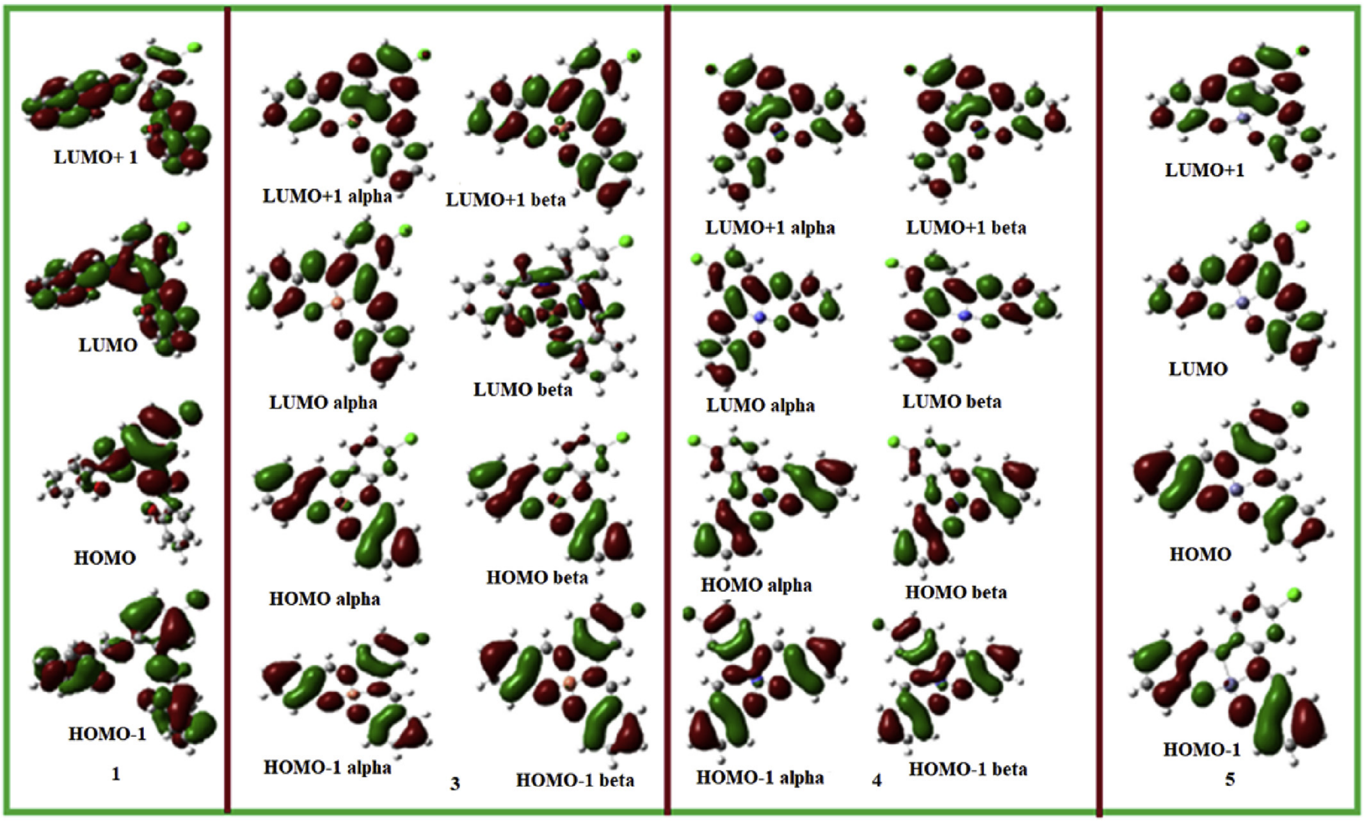

Fig. 11. Molecular orbitals for salophen ligand **1** and its complexes with copper (**3**), cobalt (**4**) and Zinc (**5**).

are stable up to 340 °C with a DTGmax = 340.12 °C for **3** and 342 °C for **6**. Decomposition for these complexes involves three steps. The weight loss in the first stage is probably related to the presence of the lattice cell water or other solvents in the complexes. The second stage can be related to the omission of CO molecule of **3** or CO_2 molecule of **6** with a mass lose 6.80% (calc. 7.33%) and 9.64% (calc.9.59%) [61]. The highest weight loss occurs in the range of 600–950 °C, which corresponds to the decomposition of the residue aromatic groups (loss of the C_7H_5O group in **3** and C_7H_5N group in **6**) with a mass lose 27.64% (Calc. 27.34%) and 24.62 (Calc. 24.96%) (Fig. 7 and Fig. S15) [60,61].

For Co (II) complex **4** and **7**, TGA curves indicate that the loss of weight starts around 121 and 127 °C (Fig. 7 and Fig. S16). The loss of weight take places in six steps for **4** and five steps for **7**. The weight loss in first stage can be corresponded to the elimination of water from lattice cell of the complexes with a mass lose 5.82% (calc. 6.21%) for **4** and 6.91% (calc. 7.37 %) for **7**. Similar to Cu(II) complexes, the second stage can be assigned to the release of CO_2 molecule of the main body of **4** and **7** with a mass lose 9.02% (calc. 10.79 %) and 8.25% (calc.9.73%), respectively. Decomposition of organic groups for compounds **4** and **7** starts from 300 °C. The first, second, third and fourth stages in the temperature range 300–700 °C, theoretically calculated weight losses for **4** are: 14.24%, 8.67%, 8.73% and 7.57%. The thermal analyses for **4** show experimentally weight losses of 14.30%, 8.03%, 8.73% and 9.56% and corresponds to the decomposition of some parts of residual aromatic rings of Schiff base ligand **1**. The first and the second stage of decomposition of the organic groups, theoretically calculated weight losses for **7** are 12.74% and 7.0%. The thermal analyses for **7** reveals experimentally weight losses of 12.39%, 5.42%. These stages involve the decomposition of one of the residual aromatic rings of the schiff base ligand **2** in two steps. The final decomposition step is related to the omission of the second residue aromatic ring of the main body of complex **7** with a mass lose 22.03% (calc. 22.96%). Zn(II) complex **5** is stable to 203.04 °C while Zn(II) complex **8** is stable to 196.3 °C. Zn (II) complexes **5** and **8** reveal four and three decomposition peaks in the thermograms (203.04 °C, 383.81 °C, 527.23 °C and 689.95 °C for **5** and 196.34 °C, 370.20 °C and 710.31 °C for **8**). The weight loss in the first stage is probably corresponds to the presence of the lattice cell or coordinated water with a mass lose 6.14% (calc. 6.12%) for **5** and a mass lose 4.92 % (calc. 4.67 %) for **8**. The second stage can be related to the omission of CO molecule of **5** with a mass lose 7.47% (calc. 6.77 %) and **8** with a mass lose 4.76% (calc. 6.10%). The highest weight loss take places about 450–950 °C that can be related to the removal of one of the phenolate groups with a mass lose 23.81% (calc. 23.86 %) for **5** and the elimination of the aromatic ring containing of bromo substitution with a mass lose 39.48 % (calc. 42.52 %) for **8** (Figs. 7 and S17).

3.7. *Biological activity*

The in vitro antibacterial activity is tested by agar well diffusion assay using *Staphylococcus aureus*, *Escherichia coli*, *Pseudomonas aeruginosa* and carbapenem &colistin resistant *Klebsiella pneumoniae*. The results of susceptibility testing, presented as diameter of the zone of inhibition are given in Table 3. As shown in Fig. 8, both Co(II) complexes **4** and **7** have remarkable antibacterial activity against *S. aureus* as a medically important Gram positive bacterium. Also, cobalt complexes **4** and **7** reveal the greatest antibacterial activity against carbapenem & colistin resistant *Klebsiella pneumoniae*. This antibacterial effect is of high interest as the bacterium, is resistant to two most important therapeutic options for treatment of multi-drug resistant Gram negative bacteria, including polymyxins and carbapenems. Moreover, Schiff-base ligands **1** and

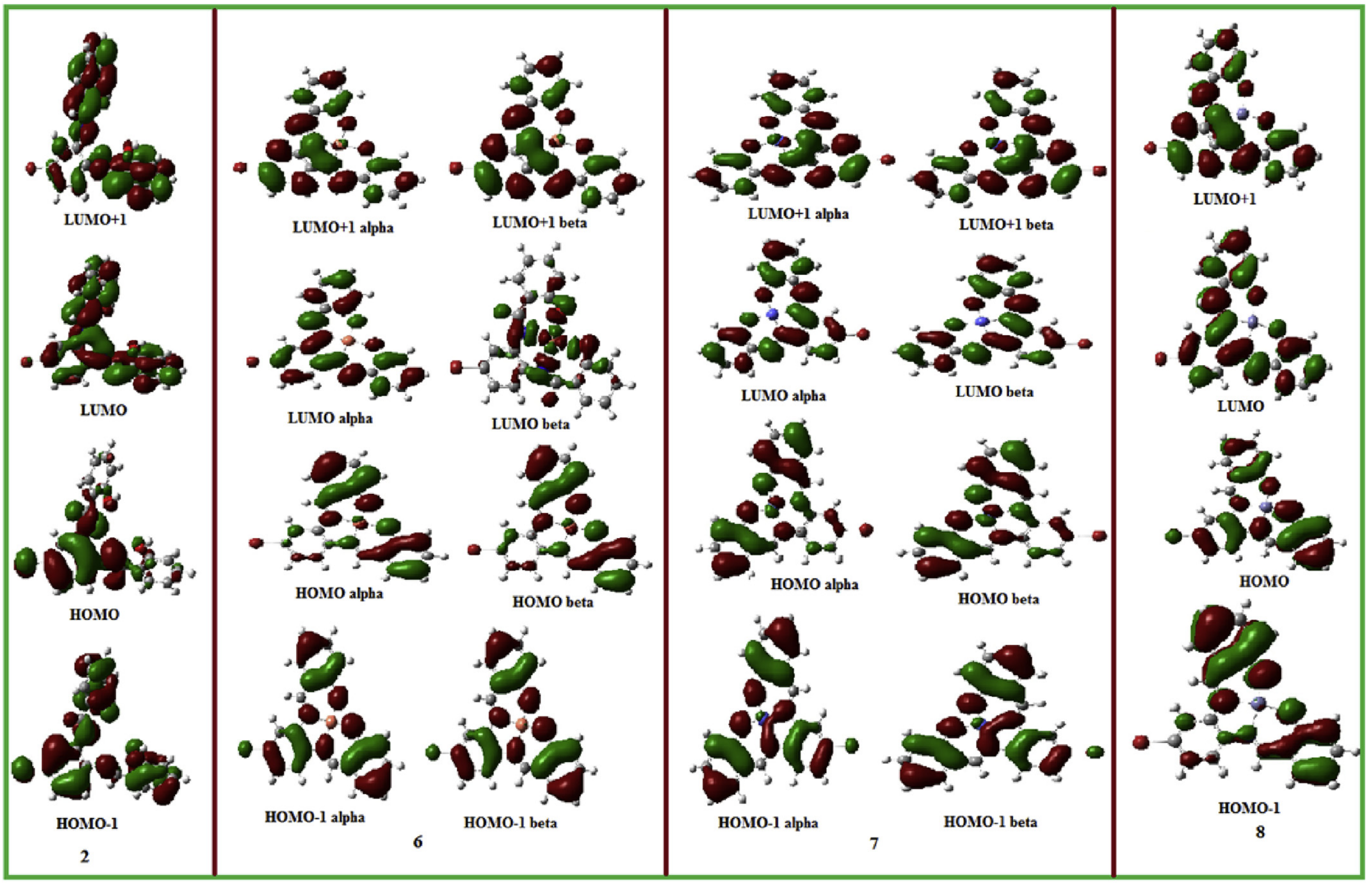

Fig. 12. Molecular orbitals for salophen ligand **2** and its complexes with copper (**6**), cobalt (**7**) and Zinc (**8**).

2 are more active than their copper and zinc complexes against studied bacteria.

3.8. *Theoretical studies*

Density Functional theory (DFT) investigations are performed to obtain a better understanding of structure and electronic properties of compounds **1**–**8**. The fully optimized molecular structures of all ligands and complexes are shown in Figs. 9 and 10. Also, molecular orbital surfaces for HOMO-1, HOMO, LUMO and LUMO+1 of ligands and their complexes are given in Figs. 11 and 12. Analysis of the frontier orbital molecules of ligands **1** and **2** indicates that the band gaps are 2.24 eV and 2.22 eV, respectively. The band gaps for Cu(II) complexes **3** and **6**, Co(II) complexes **4** and **7** and Zn(II) complexes **6** and **8** have similar values: 1.92 eV (alpha) and 1.88 eV (beta), 1.82 eV (alpha), 1.77 eV (beta) and 1.94 eV. The band gap values of all complexes shows their potential ability for using in optical devices such as solar cells.

3.8.1. *UV–vis spectra by TD-DFT calculations*

TD-DFT calculations are performed on ground state of optimized their structures to predict electronic spectra of compounds **1**–**8**. Some electronic transitions for ligands and complexes have been given in Tables S1–S8 from Supplemental Material.

3.8.1.1. Ligands. The simulated spectra of both ligands are given in Fig. S18. To analyze the theoretical spectra, the calculated transitions with major oscillator strength are considered. The tenth excited state for ligand **1** and the eighth excited state for ligand **2** are due to the excitation of electron from HOMO → LUMO+2 (50%) and HOMO-5 → LUMO (64%), respectively. The maximum localization of the HOMO and HOMO-5 are on π(C) orbitals and iminc bonds while the LUMO+2 of **1** is mainly consist of π* orbitals of aromatic rings and the LUMO of **2** includes the π* orbitals expanded on aromatic ring and iminic bonds. This transition can be attributed to the $\pi \rightarrow \pi^*$ of aromatic rings. The second excited state for ligands **1** and **2** are due to HOMO → LUMO+1 (92%) and HOMO-1 → LUMO (~75%). HOMO-1 of both ligands is mainly formed of π(C) orbitals and iminc bands, while the maximum localization of the LUMO+1of **1** and the LUMO of **2** is on π* orbitals of aromatic rings and iminc bands. Therefore, these transitions can be attributed to the $\pi \rightarrow \pi^*$ of aromatic rings and $n \rightarrow \pi^*$ of azomethine bonds. Finally, the first excited state of ligands **1** and **2** which related to the promotion of electron from HOMO → LUMO (95%), can be assigned to the intra-ligand transitions.

3.8.1.2. Complexes. The simulated spectra of all complexes are shown in Figs. S19 and S20. To investigate the theoretical spectra, the calculated transitions with major oscillator strength are considered. In all complexes, the high energy bands are associated to the intra-ligand transitions ($\pi \rightarrow \pi^*$ and $n \rightarrow \pi^*$). The low energy bands of Cu complex **3** and **6** originate mainly from intra-ligand transitions and to lesser extend from MLCT($Cu \rightarrow \pi^*$) or LMCT ($\pi \rightarrow Cu$) transitions. The low energy bands of Co complexes **4** and **7** corresponds to MLCT $Co \rightarrow \pi^*$ type and intra-ligand transition and to lesser expand from LMCT. While, the low energy bands of Zn complexes **5** and **8** is mainly related to the intra-ligand transitions. Generally, the theoretical data reveal the good agreement with the experimental data compared to the literature which are used the TD-DFT method at the B3LYP/LANL2DZ level for calculation of the excited state properties of complexes [62–67].

4. Conclusions

In this study, copper, cobalt and zinc complexes with salophen type ligands containing chlorine and bromine were synthesized. All compounds were fully characterized and their optical, electrochemical, thermal and antibacterial activity investigated. UV–Vis spectra of all complexes showed the absorption bands in the 400–500 nm region which related to the $\pi \rightarrow \pi^*$ transitions of keto forms of ligands (and also metal to ligand charge transfer for Cu(II) and Co(II) complexes). Ligands **1** and **2** exhibited one maximum emission peak at 476 nm due to ESIPT phenomenon and also intraligand $\pi \rightarrow \pi^*$ transitions. The results showed that all of complexes quench the fluorescence of ligands which means that none of the absorption peaks leads to a noticeable emission in the complexes compared to the free ligands. The cyclic voltammogrames of Cu (II) and Co(II) complexes presented one quasi-reversible redox couple of Cu(II)/Cu(I) and two fine reversible redox couples of Co(II)/Co(I) and Co(III)/Co (II), respectively. The investigation of antibacterial activity by agar well diffusion assay showed the Co(II) complexes **4** and **7** have one strong antibacterial effect upon the studies bacteria. Finally, the molecular geometry of Schiff base ligands and their complexes in the ground state was obtained by DFT calculations. Based on optimized structures, electronic absorption spectra of the ligands and complexes were simulated by TD-DFT method that displayed good agreement with the experimental data. This study would pave the way for using of these complexes in several fields such as precursors for preparation of metal oxide nanostructures, photovoltaic, electrocatalytic (water oxidation) and biological applications for future works.

Acknowledgements

The authors are grateful to Azarbaijan Shahid Madani University and Tabriz University for financial support of this study. Also, the authors thank Dr. Ardavan Masoudiasl for helping to the theoretical studies.

Appendix A. Supplementary data

Supplementary data to this article can be found online at https://doi.org/10.1016/j.molstruc.2019.127107.

References

[1] P.A. Vigato, S. Tamburini, The challenge of cyclic and acyclic schiff bases and related derivatives, Coord. Chem. Rev. 248 (2004) 1717–2128.
[2] P. Pfeiffer, E. Breith, E. Lubbe, T. Tsumaki, Justus Liebigs, N,N'-ethylenebis(salicylideneiminato) transition metal ion chelates, Ann. Chem. 503 (1933) 84–130.
[3] F. Sabaté, R. Gavara, I. Giannicchi, R. Bosque, A.D. Cort, L. Rodrıguez, Ternary assemblies comprising metal–salophen complexes and 4,4′-bipyridine, New J. Chem. 40 (2016) 5714–5721.
[4] W.A. Zoubi, Y.G. Ko, Organometallic complexes of Schiff bases: recent progress in oxidation catalysis, J. Organomet. Chem. 822 (2016) 173–188.
[5] J. Wöltinger, J.E. Bäckvall, A. Zsigmond, Zeolite-encapsulated cobalt salophen complexes as efficient oxygen-activating catalysts in palladium-catalyzed aerobic 1,4-oxidation of 1,3-dienes, Chem. Eur J. 5 (1999) 1460–1467.
[6] J. Jiang, K. Ma, Y. Zheng, S. Cai, R. Li, J. Ma, Cobalt salophen complex immobilized into montmorillanite as catalyst for the epoxidation of cyclohexene by air, Appl. Clay Sci. 45 (2009) 117–122.
[7] F. Wu, C.J. Wang, H. Lin, A.Q. Jia, Q.F. Zhang, Syntheses, structures and catalytic properties of ruthenium(II) nitrosyl complexes with bidentate and tetradentate Schiff base ligands, Inorg. Chim. Acta 471 (2018) 718–723.
[8] V. Mirkhani, M. Moghadam, S. Tangestaninejad, B. Bahramian, A. Mallekpoor-Shalamzari, Host (nanocavity of zeolite-Y)–guest (manganese(III) salophen complex) nanocomposite materials: an efficient catalyst for biomimetic alkene epoxidation and alkane hydroxylation with sodium periodate, Appl. Catal., A 321 (2007) 49–57.
[9] J.A. Castro-Osma, K.J. Lamb, M. North, Cr(salophen) complex catalyzed cyclic carbonate synthesis at ambient temperature and pressure, ACS Catal. 6 (2016) 5012–5025.
[10] T. Wu, T. Wang, L. Sun, K. Deng, W. Deng, R. Lu, A DFT exploration of efficient catalysts based on metal-salen monomers for the cycloaddition reaction of CO_2 to propylene oxide, ChemistrySelect 2 (2017) 4533–4537.
[11] J. Chun, S. Kang, N. Kang, S.M. Lee, H.G. Kim, S.U. Son, Microporous organic networks bearing metal-salen species for mild CO_2 fixation to cyclic carbonates, J. Mater. Chem. 1 (2013) 5517–5523.
[12] S. Di Bella, I.P. Oliveri, A. Colombo, C. Dragonetti, S. Righetto, D. Roberto, An unprecedented switching of the second-order nonlinear optical response in aggregate bis(salicylaldiminato)zinc(II) Schiff-base complexes, Dalton Trans. 41 (2012) 7013–7016.
[13] H. Uh, P.D. Badger, S.J. Geib, S. Petoud, Synthesis and solid-state, solution, and luminescence properties of near-infrared-emitting neodymium(3+) complexes formed with ligands derived from salophen, Helv. Chim. Acta 92 (2009) 2313–2329.
[14] C. Ma, A. Lo, A. Abdolmaleki, M.J. MacLachlan, Synthesis and metalation of novel fluorescent conjugated macrocycles, Org. Lett. 6 (2004) 3841–3844.
[15] T.M. Fasina, O. Ogundele, F.N. Ejiah, C.U. Dueke-Eze, Biological activity of copper (II), cobalt (II) and nickel (II) complexes of schiff base derived from O-phenylenediamine and 5-bromosalicylaldehyde, Int. J. Biol. Chem. 6 (2012) 24–30.
[16] R. Brissos, D. Ramos, J.C. Lima, F.Y. Mihan, M. Borràs, J.d. Lapuente, A.D. Cort, L. Rodríguez, Luminescent zinc salophen derivatives: cytotoxicity assessment and action mechanism studies, New J. Chem. 37 (2013) 1046–1055.
[17] M. Mahato, D. Dey, S. Pal, S. Saha, A. Ghosh, K. Harms, H.P. Nayek, Syntheses, structures, optical properties and biological activities of bimetallic complexes, RSC Adv. 4 (2014) 64725–64730.
[18] U. Patil, M. Mandewale1, B. Thorat1, A. Nagarsekar, R. Yamgar, Transition metal tetrahydro-salophen type complexes: synthesis, characterization and antitubercular studies, Asian J. Res. Chem. 9 (2016) 425–434.
[19] L. Lecarme, E. Prado, A. De Rache, M.L.N. Travers, R. Bonnet, A.V.D. Heyden, C. Philouze, D. Gomez, J.L. Mergny, H. Jamet, E. Defrancq, O. Jarjayes, F. Thomas, Interaction of polycationic Ni(II)-Salophen complexes with G-quadruplex DNA, Inorg. Chem. 53 (2014) 12519–12531.
[20] S. Majumder, S. Pasayat, A.K. Panda, S.P. Dash, S. Roy, A. Biswas, M.E. Varma, B.N. Joshi, E. Garribba, C. Kausar, S.K. Patra, W. Kaminsky, A. Crochet, R. Dinda, Monomeric and dimeric oxidomolybdenum(V and VI) complexes, cytotoxicity, and DNA interaction studies: molybdenum assisted C═N bond cleavage of salophen ligands, Inorg. Chem. 56 (2017) 11190–11210.
[21] A.D. Cort, P.D. Bernardin, G. Forte, F.Y. Mihan, Metal–salophen-based receptors for anions, Chem. Soc. Rev. 39 (2010) 3863–3874.
[22] E. Bodo, A. Ciavardini, A.D. 14;Cort, I. Giannicchi, F.Y. 14;Mihan, S. Fornarini, S. Vasile, D. Scuderi, S. Piccirillo, Anion recognition by uranyl–salophen derivatives as probed by infrared multiple photon dissociation spectroscopy and ab initio modeling, Chem. Eur J. 20 (2014) 11783–11792.
[23] L. Leoni, R. Puttreddy, O. Jurček, A. Mele, I. Giannicchi, F.Y. Mihan, K. Rissanen, A.D. 14;Cort, Solution and solid-state studies on the halide binding affinity of perfluorophenyl-armed uranyl–salophen receptors enhanced by anion–π interactions, Chem. Eur J. 22 (2016) 18714–18717.
[24] I. Giannicchi, R. Brissos, D. Ramos, J.d. Lapuente, J.C. Lima, A.D. Cort, L. Rodríguez, Substituent effects on the biological properties of Zn-salophen complexes, Inorg. Chem. 52 (2013) 9245–9253.
[25] A. Arola-Arnal, J. Benet-Buchholz, S. Neidle, R. Vilar, Effects of metal coordination geometry on stabilization of human telomeric quadruplex DNA by square-planar and square-pyramidal metal complexes, Inorg. Chem. 47 (2008) 11910–11919.
[26] M. Cano, L. Rodríguez, J.C. Lima, F. Pina, A.D. Cort, C. Pasquini, L. Schiaffino, Specific supramolecular interactions between Zn^{2+}-salophen complexes and biologically relevant anions, Inorg. Chem. 48 (2009) 6229–6235.
[27] M.E. Germain, T.R. Vargo, B.A. McClure, J.J. Rack, P.G. Van Patten, M. Odoi, M.J. Knapp, Quenching mechanism of Zn(salicylaldimine) by nitroaromatics, Inorg. Chem. 47 (2008) 6203–6211.
[28] A. Dalla Cort, L. Mandolini, C. Pasquini, K. Rissanen, L. Russob, L. Schiaffinoa, Zinc–salophen complexes as selective receptors for tertiary amines, New J. Chem. 31 (2007) 1633–1638.
[29] G. Consiglio, S. Failla, P. Finocchiaro, I.P. Oliveri, S. Di Bella, Aggregation properties of bis(salicylaldiminato)zinc(II) Schiff-base complexes and their Lewis acidic character, Dalton Trans. 41 (2012) 387–395.
[30] C.W. Anson, S.S. Stahl, Cooperative electrocatalytic O_2 reduction involving Co(salophen) with *p*-hydroquinone as an electron–proton transfer mediator, J. Am. Chem. Soc. 139 (2017) 18472–18475.
[31] M.A. Asraf, H.A. Younus, C.I. Ezugwu, A. Mehta, F. Verpoort, Cobalt salophen complexes for light-driven water oxidation, Catal. Sci. Technol. 6 (2016) 4271–4282.
[32] M. Benjamin, D. Manoj, K. Thenmozhi, P.R. Bhagat, D. Saravanakumar, S. Senthilkumar, A bioinspired ionic liquid tagged cobalt-salophen complex for nonenzymatic detection of glucose, Biosens. Bioelectron. 91 (2017) 380–387.
[33] H. Khoshro, H.R. Zare, A. Gorji, M. Namazian, A.A. Jafari, R. Vafazadeh, The effect of electronic structure on electrocatalytic behaviors of cobalt Schiff base complexes: electrosynthesis of 2-phenylacetic acid using carbon dioxide,

J. Electroanal. Chem. 732 (2014) 117–121.

[34] A. Kocak, H. Yilmaz, O. Faiz, O. Andac, Experimental and theoretical studies on Cu(II) complex of N,N′-disalicylidene-2,3-diaminopyridine ligand reveal indirect evidence for DNA intercalation, Polyhedron 104 (2016) 106–115.

[35] P.R. Reddy, A. Shilpa, Synthesis, characterization, and DNA-binding and -cleavage properties of dinuclear Cu^{II}-Salophen/Salen complexes, Chem. Biodivers. 8 (2011) 1245–1265.

[36] J. Cisterna, V. Artigas, M. Fuentealba, P. Hamon, C. Manzur, V. Dorcet, J.-R. Hamon, D. Carrillo, Nickel(II) and copper(II) complexes of new unsymmetrically-substituted tetradentate Schiff base ligands: spectral, structural, electrochemical and computational studies, Inorg. Chim. Acta 462 (2017) 266–280.

[37] G. Consiglio, S. Failla, C.G. Fortuna, L. D'Urso, G. Forte, Aggregation of a Zn(II)-salen complex: theoretical study of structure and spectra, Comput. Theor. Chem. 1067 (2015) 1–6.

[38] S.A. Zarei, A mononuclear cobalt(II) salophen-type complex: synthesis, theoretical and experimental electronic absorption and infrared spectra, crystal structure, and predicting of second- and third-order nonlinear optical properties, Spectrochim. Acta, Part A 215 (2019) 225–232.

[39] P. Zanelio, A. Cinquantini, Electrochemical behaviour of a series of N,N′-1,2-Phenylenebis(salicylideneimin)ato transition metal complexes, Trans. Met. Chem. 10 (1985) 370–374.

[40] J. Gao, Y. Cheng, 2,2'-[5-Bromo-o-phenylenebis(nitrilomethylidyne)]Diphenol, Acta Crystallogr. E65 (2009) o979.

[41] M.J. Frisch, et al., Gaussian 09, Revision D.01, Gaussian InC, Wallingford CT, 2004.

[42] C. Lee, W. Yang, R.G. Parr, Phys. Rev. B 17 (1988) 785–789.

[43] E. Gross, W. Kohn, Adv. Quant. Chem. 21 (1990) 255–291.

[44] A.N. Kursunlu, E. Guler, F. Sevgi, B. Ozkalp, Synthesis, spectroscopic characterization and antimicrobial studies of Co(II), Ni(II), Cu(II) and Zn(II) complexes with Schiff bases derived from 5-bromo-salicylaldehyde, J. Mol. Struct. 1048 (2013) 476–481.

[45] M.S. More, S.B. Pawal, S.R. Lolage, S.S. Chavan, Syntheses, structural characterization, luminescence and optical studies of Ni(II) and Zn(II) complexes containing salophen ligand, J. Mol. Struct. 1128 (2017) 419–427.

[46] S. Demir, H. Yılmaz, M. Dilimulati, M. Andac, Spectral and thermal characterization of salophen type Schiff base and its implementation as solid contact electrode for quantitative monitoring of copper(II) ion, Spectrochim. Acta, Part A 150 (2015) 523–532.

[47] A. Ourari, K. Ouari, W. Moumeni, L.S. Gilles, M. Bouet, M.A. Khan, Unsymmetrical tetradentate schiff base complexes derived from 2,3-diaminophenol and salicylaldehyde or 5-bromosalicylaldehyde, Trans. Met. Chem. 31 (2006) 169–175.

[48] K.-L. Kuo, C.-C. Huang, Y.-C. Lin, Synthesis and photophysical properties of multinuclear zinc-salophen complexes: enhancement of fluorescence by fluorene termini, Dalton Trans. (2008) 3889–3898.

[49] M. Ziółek, J. Kubicki, A. Maciejewski, R. Naskrecki, A. Grabowska, Enol-keto tautomerism of aromatic photochromic Schiff base N,N′-bis(salicylidene)-p-phenylenediamine: ground state equilibrium and excited state deactivation studied by solvatochromic measurements on ultrafast time scale, J. Chem. Phys. 124 (2006), 124518-10.

[50] T. Khan, S. Vaidya, D.S. Mhatre, A. Datta, The prospect of salophen in fluorescence lifetime sensing of Al^{3+}, J. Phys. Chem. B 120 (2016) 10319–10326.

[51] K.T. Smith, S.C. Young, G.W. DeBlasio, C.S. Hamann, Measuring structural and electronic effects on keto–enol equilibrium in 1,3-dicarbonyl compounds, J. Chem. Educ. 93 (2016) 790.

[52] E. Tas, V.T. Kasumov, O. Sahin, M. Ozdemir, Transition metal complexes with tridentate salicylaldimine derived from 3,5-di-t-butylsalicylaldehyde, Transition Met. Chem. 27 (2002) 442–446.

[53] B. Ortiz, S.-M. Park, Electrochemical and spectroelectrochemical studies of cobalt salen and salophen as oxygen reduction catalysts, Bull. Korean Chem. Soc. 21 (2000) 405–411.

[54] C. Fraser, B. Bosnich, Bimetallic reactivity, investigation of metal-metal interaction in complexes of a chiral macrocyclic binucleating ligand bearing 6- and 4-coordinate sites, Inorg. Chem. 33 (1994) 338–346.

[55] C.M. Sharaby, Synthesis, spectroscopic, thermal and antimicrobial studies of some novel metal complexes of Schiff base derived from [N1-(4-methoxy-1,2,5-thiadiazol-3-yl)sulfanilamide] and 2-thiophene carboxaldehyde, Spectrochim. Acta, Part A 66 (2007) 1271–1278.

[56] W. Rodríguez-Córdoba, J.S. Zugazagoitia, E. Collado-Fregoso, J. Peon, Excited state intramolecular proton transfer in schiff bases. Decay of the locally excited enol state observed by femtosecond resolved fluorescence, J. Phys. Chem. A 111 (2007) 6241–6247.

[57] J.M. Ortiz-Sánchez, R. Gelabert, M. Moreno, J.M. Lluch, Theoretical study on the excited-state intramolecular proton transfer in the aromatic schiff base salicylidene Methylamine: an electronic structure and quantum dynamical approach, J. Phys. Chem. A 110 (2007) 4649–4656.

[58] M.G. Vivas, J.C. Germino, C.A. Barboza, D. de A. Simoni, P.A.M. Vazquez, L. De Boni, T.D.Z. Atvars, C.R. Mendonça, Revealing the dynamic of excited state proton transfer of a π-conjugated salicylidene compound: an experimental and theoretical study, J. Phys. Chem. C 121 (2017) 1283–1290.

[59] N.J. Turro, Energy transfer processes, Pure Appl. Chem. 49 (1977) 405–429.

[60] T. Ueda, N. Inazuma, D. Komatsu, H. Yasuzawa, A. Onda, S.X. Guoc, A.M. Bond, Comparison of chemical interactions with Li^{+} and catalytic reactivity of electrochemically generated [Fe^{I}Cl(L)]$^{2-}$ and [Co^{I}(L)]$^{-}$ complexes (L = salen or salophen), Dalton Trans. 42 (2013) 11146–11154.

[61] S. Uysal, Z.E. Koç, The synthesis and characterization of (MSalen/salophen/saldeta/salpy) [M=Fe(III) or Cr(III)] capped heteromultinuclear schiff bases-dioxime Ni(II) complexes: their thermal and magnetic behaviours, J. Mol. Struct. 1165 (2018) 14–22.

[62] S. Celikbilek, Z.E. Koc, Investigation of Dipodal oxy-Schiff base and its salen and salophen Fe(III)/Cr(III)/Mn(III) Schiff bases (N_2O_2) caped complexes and their magnetic and thermal behaviors, J. Mol. Struct. 1065–1066 (2014) 205–209.

[63] S.G. Niyaky, M. Montazerozohori, A. Masoudiasl, J.M. White, New five coordinated supramolecular structured cadmium complex as precursor for CdO nanoparticles: synthesis, crystal structure, theoretical and 3D Hirshfeld surface analyses, J. Mol. Struct. 1131 (2017) 201–211.

[64] K. Nejati, A. Bakhtiari, R. Bikas, J. Rahimpour, Molecular and electronic structure, spectroscopic and electrochemical properties of Copper(II) complexes: experimental and DFT studies, J. Mol. Struct. 1192 (2019) 217–229.

[65] A. Masoudiasla, M. Montazerozohoria, S. Jooharib, L. Taghizadeha, G. Mahmoudic, A. Assoudd, Structural investigation of a new cadmium coordination compound prepared by sonochemical process: crystal structure, Hirshfeld surface, thermal, TD-DFT and NBO analyses, Ultrason. Sonochem. 52 (2019) 244–256.

[66] H. Gökce, B. Dede, S. Bahçeli, Structural, spectroscopic and quantum chemical studies on copper(II) complex of 4-ethoxy-2-methyl-5-(4-morpholinyl)-3(2H)-pyridazinone, J. Mol. Struct. 1171 (2018) 471–480.

[67] G. Görgülü, B. Dede, Synthesis, characterization, theoretical calculations and biochemical evaluation of a novel oxime ligand with complexes, J. Mol. Liq. 284 (2019) 473–491.